Lipid domains as obstacles for lateral diffusion in supported bilayers probed at different time and length scales by two-dimensional exchange and field gradient solid state NMR

C. Dolainsky,[1] P. Karakatsanis,[1] and T. M. Bayerl[2,*]
[1]*Technische Universität München, Physik Department E22, D-85747 Garching, Germany*
[2]*Universität Würzburg, Physikalisches Institut EP-V, D-97074 Würzburg, Germany*
(Received 1 August 1996)

Employing two new solid-state NMR techniques for measuring lateral diffusion of lipids in supported bilayers, the deuterium two-dimensional exchange deuterium NMR (2D-NMR) and the Supercon fringe field proton NMR, we have studied bilayer domain connectivity in the coexistence region of a 1:1 DMPC-DSPC mixture. The advantage of the NMR methods is that they permit the study of percolation in lipid mixtures as a function of the experimental time and length scale and that they do not rely on the use of any labels attached to the lipids that change their molecular packing properties. Both NMR methods show an excellent agreement of their results at comparable mixing times. Moreover, a simulation of the effect of restricted diffusion on the 2D-NMR spectra shows clearly that the sensitivity of 2D-NMR for gel domains as diffusion obstacles in terms of a simple domain model depends on the mixing time and thus on the length scale of the experiment. In contrast to previous findings made by fluorescence and spin label studies, we do not observe any discontinuity of the lateral diffusion coefficient D indicative of a disconnection of the fluid phase down to a temperature which is only 4 °C above the solidus temperature of the mixture. At experimental length scales below 200 nm, D is not significantly reduced due to the presence of gel phase domains up to an area fraction of 0.5. At length scales between 500 nm and 1 μm both methods give a rather linear decrease of D with increasing gel phase area fraction, starting in the vicinity of the liquidus point. This surprising result is discussed in terms of the relationship between experimental length scale and detectability of percolation. [S1063-651X(97)04904-0]

PACS number(s): 87.15.−v

I. INTRODUCTION

Measurements of lipid lateral diffusion in bilayers are well established for a wide variety of synthetic and natural lipids, mainly by fluorescence (FRAP, cf. [1] for review) [2], NMR [3–5], electron spin resonance (ESR) [6–8], and, more recently, neutron scattering methods [9,10]. These measurements, performed mostly in bilayers consisting of just one lipid species, provided ample evidence for the validity of the free volume model of lateral diffusion [2]. However, things get more complicated when diffusion measurements are performed in binary lipid mixtures under conditions that fluid and gel phases exist simultaneously, i.e., in the coexistence region of their phase diagram. The spontaneous occurrence of gel phase domains in which no lateral diffusion takes place, at temperatures in the vicinity of the liquidus line certainly represents an obstacle for unrestricted two-dimensional diffusion in the plane of the bilayer. With decreasing temperature, such gel domains grow either in size or number (or both) and the surrounding fluid becomes finally disconnected at a certain temperature T_D. This point, at which the disconnected gel existing at temperatures T above T_D changes to a disconnected fluid for $T<T_D$ should be observable by a marked reduction of long-range lipid diffusion. Indeed, this has been established by FRAP [1,11,12] and ESR [13] measurements and both methods gave $T_D=(43\pm2)$ °C, close to the liquidus temperature, for an equimolar DMPC-DSPC mixture. The fact that both methods provided the same value for T_D is a little surprising since they should be sensitive at very different time and length scales. For example, if the size of the disconnected fluid is less than the length over which the method is sensitive, a drop in the measured long-range diffusion within the fluid should be readily detectable. Thus it seems that T_D measured by a certain method should depend on its characteristic length scale, although the above mentioned FRAP and ESR measurements on DMPC-DSPC do not confirm this surmise.

Over recent years we have developed a number of sensitive solid-state NMR [4,5,14] and dynamic neutron scattering [15] methods that allow quantitative measurements of lipid lateral diffusion over very different length scales, ranging from 10 Å up to 1–2 μm. The aim of this work is to employ two of these methods for studying the dependence of disconnection phenomena in equimolar DMPC-DSPC mixtures on the experimental time and length scale and to resolve the question about a T_D dependence on it. We have chosen the two-dimensional exchange deuterium NMR (2D-NMR) and the Supercon fringe field gradient (SFF) technique to measure the diffusion at different length scales ranging from 200 nm to 1 μm. Beside the adjustability of time and length scales our methods have another clear advantage over FRAP and ESR insofar as they do not rely on the use of labels that change the molecular packing properties of the probe molecules compared to that of the bulk lipids.

*Fax: 49-931-888-5851. Electronic address: tbayerl@physik.tu-muenchen.de

II. MATERIALS AND METHODS

A. Preparation of samples and calorimetry

1,2-di-stearoyl-*sn*-glycero-3-phosphatidyl-choline (DSPC), 1,2-di-stearoyl-*d*70-*sn*-glycero-3-phosphatidyl-choline (DSPC-*d*70) 1,2-di-myristoyl-*d*54-*sn*-glycero-3-phosphatidyl-choline (DMPC-*d*54), and the head group labeled 1,2-di-myristoyl-*sn*-glycero-3-phosphatidyl-choline-*N*,*N*,*N*-trimethyl-*d*9 (DMPC-*d*9) were purchased from Avanti Polar Lipids (Alabaster, AL). Deuterium-depleted water from Isotec Inc. (Miamisburg, OH) was used for the preparation of multilamellar vesicles (MLV) to prevent the isotropic water line. Ultrapure D_2O used for the SFF measurements was from Deuchem GmbH (Leipzig, Germany). The solvents (Chloroform and Methanol) were purchased in HPLC quality from Merck (Darmstadt, Germany). Silica spheres used as solid support were obtained from Degussa (Hanau, Germany) and have a radius of 320 ± 20 nm and a microscopic surface roughness of less than 3 Å.

Single bilayers of DMPC-*d*9 on a spherical support of silica were prepared as described previously [16]. The preparation of the binary DSPC-DMPC-*d*9 mixture was quite analogous and is described in detail in [17]. For both preparation procedures the final sample was dispersed in deuterium-depleted water at a concentration of $\approx$10 mg lipid/ml and transferred into 1-ml-plastic NMR sample caps of 10-mm-diam. For SFF proton NMR measurements, planar-oriented lipid multilayers of 1:1 DMPC–*d*54–DSPC-*d*70 were prepared according to a procedure described in detail in [14] and hydrated with D_2O via the vapor phase to give a final hydration of 30 wt %. A sample consists of 70 stacked glass plates as a substrate, 2×12.5 mm each, with a total amount of 30 mg lipid.

The orientation of the membrane normal was perpendicular to the field gradient for the diffusion measurement.

The temperatures of liquidus and solidus points of the NMR samples were checked after the NMR experiments by running heating scans using a differential scanning calorimeter from Hart Scientific Inc. (Salt Lake City, UT). No changes of these temperatures were detected compared to control samples.

B. NMR experiments

The 2D-exchange deuterium NMR (2D-NMR) experiments and Supercon fringe field (SFF) proton NMR measurements were performed on a Varian VXR 400 spectrometer (Varian, Palo Alto, CA) equipped with a 10-mm-high power broadline probe operating at 61.395 MHz (for deuterons) and at 214.0 MHz (for protons under SFF conditions).

1. 2D-NMR

For 2D-NMR, the 90 °C pulse was 6 μs and 512 scans were acquired with a recycle delay of 250 ms, using a pulse sequence presented by Schmidt, Blümich, and Spiess [18]: 90_y-t_1-ψ_ϕ-t_m-$\psi_{\phi'}$-τ-90_x-τ-t_2. To achieve quadrature detection in t_1 the phase cycling scheme as described in [18] was used and expanded to account for imperfections of the last pulse [5]. Furthermore, $\psi=90°$ pulses were used for the sine experiment and $\psi=45°$ pulses for the cosine experiment instead of the 54.7° ϕ pulses described by [18]. Thus a weighting factor of 1.33 had to be applied to the time domain data of the cosine experiment prior Fourier transformation to account for the intensity difference. 128 t_1 and 256 complex t_2 values were acquired in each experiment with a dwell time of 25 μs. The refocusing delay τ was 100 μs. Experiments with mixing times t_m of 2, 4, 6, and 12 ms were performed.

The experiments started at a temperature of 55 °C after an equilibration period of 30 min. The temperature was then lowered to 25 °C in steps of 3 °C. The experiments for all four mixing times at a given temperature were started 20 min after the temperature step. The temperature was maintained constant within ±1 °C using the built-in temperature control unit of the Varian spectrometer. The spectra were obtained after exponential and sinusoidal weighting of the time domain data, zero filling to 512 points and zeroth-order baseline correction in f_1 using the Fourier transform procedure described by [18].

2. SFF-NMR

The magnetic field gradient was 58 T/m at the sample site, corresponding to a sample position of 22 cm below its usual position in the homogeneous field. Diffusion of the lipid molecules of the mixture were measured using a stimulated echo sequence 90_y-τ_1-90_y-τ_2-90_y-τ_1 echo as described previously [14]. The τ_1 values were in the range from 20 to 60 μs and τ_2 values were chosen to give a reasonable echo decay. 300 transients were acquired for each echo amplitude with a 2 s repetition time. The sample contained $\approx$30 mg total lipid and was placed at the sample site at 90° orientation between membrane normal and the direction of the field gradient.

C. Simulations

For a quantitative analysis of the experimental 2D-NMR data, the results of a random walk simulation of diffusion on a sphere were required for comparison and calibration. Here a previously described simulation technique [5,19] is extended for a two-dimensional experiment and the parameters were chosen as close to the actual experiment as possible. 128 t_1 values and 256 t_2 values with a dwell time of 25 μs were simulated with mixing times of 2, 4, 6, and 12 ms. First of all the radius **R** was fixed at 320 nm. The diffusion coefficient was varied in the range of $(0.2-8)\times10^{-12}$ m^2/s, which corresponds to a diffusion correlation time (τ_D) range from 85 to 2 ms where τ_D is defined by

$$\tau_D=R^2/6D. \tag{1}$$

Furthermore, a refocusing echo sequence was simulated at the end of the 2D-NMR pulse train with a pulse spacing of 100 μs, as used in the experiments. An axially symmetric

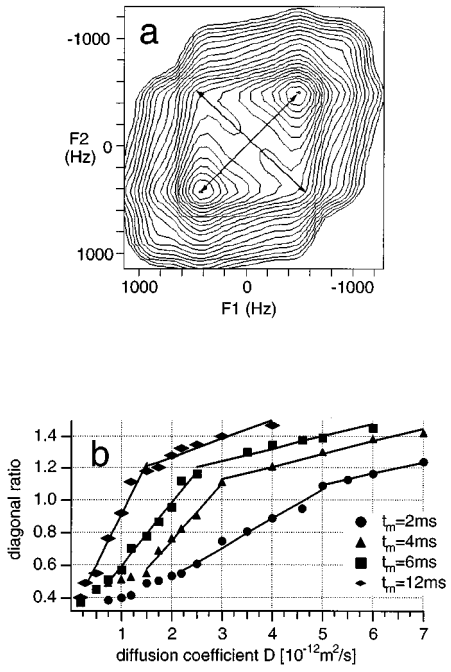

FIG. 1. (a) Determination of the diagonal ratio from the contour plot of a simulated 2D-NMR spectrum ($t_m=4$ ms, $\tau_D=5.69$ ms, $D=3\times10^{-12}$ m^2/s, and $R=320$ nm). (b) Diagonal ratios of 2D exchange spectra obtained from diffusion simulations and determined as shown in (a). Diffusional motion of deuterium spins on a sphere of 320 nm radius with diffusion coefficients D in the range 0.25×10^{-12} m^2/s to 8×10^{-12} m^2/s was simulated with a static quadrupolar splitting of 1.1 kHz and mixing times of $t_m=2$, 4, 6, and 12 ms.

quadrupolar interaction was assumed with a static quadrupolar splitting of 1.1 kHz. Due to diffusion on a curved surface this splitting was averaged out to 0.8 kHz for $D=8\times10^{-12}$ m^2/s ($\tau_D=2.1$ ms) and to 0.93 kHz for $D=1\times10^{-12}$ m^2/s ($\tau_D=17$ ms). A 200 Hz Lorentzian line broadening and a sinusoidal weighting was applied in both time domains and the same Fourier transform procedure as with the experimental data was followed.

D. Analysis of 2D spectra

In the case of DMPC-*d*9 single bilayer on a spherical support of 320 nm radius, a direct reconstruction of motional parameters as suggested by Hagemeyer *et al.* [20] and applied to lipid membranes as in [5] is not possible. The main prerequisite in this case was the assumption of slow motions, which means $t_1/\tau_D \ll 1$ and $t_2/\tau_D \ll 1$. Therefore we followed a semiempirical approach for the quantitative analysis of the DMPC-*d*9 2D-exchange deuterium NMR spectra as suggested by Fenske and Jarrell [21] together with our results from random walk simulations.

This approach uses the ratio of the length of the diagonal with respect to the length of the antidiagonal in the 2D spectra [Fig. 1(a)]. This ratio is a function of the ratio of the mixing time with respect to the correlation time of the dominating motional process in the sample. As was shown by [5], diffusion on a spherical surface is the dominating motional process in the supported systems used in this work. Therefore we can determine a diffusion coefficient by comparing

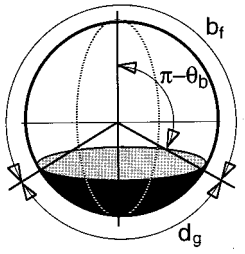

FIG. 2. Model of a gel domain (dark area) on a sphere used to calculate the effective diffusion coefficient D_{eff} from a numerical solution of a discretized boundary value problem of the spherical diffusion equation.

the diagonal ratio of simulations and 2D-NMR experiments, since the radius of the sample is in both cases well defined.

The determination of the diagonal lengths is shown in Fig. 1(a). The contour plots of spectra normalized to unity volume are used and the length of the antidiagonal is defined by the contour line at 10% of maximum intensity. It is obvious from this procedure, that very similar line-shape parameters and Fourier transformation procedures have to be applied to both experiment and simulation. The length of the diagonal is determined by the quadrupolar splitting. The simulation results in Fig. 1(b) provide a calibration curve that allows the calculation of D from the diagonal ratio. One can clearly see that the four different mixing times t_m are sensitive only for a limited range of correlation times or diffusion coefficients. The diagonal ratio of the spectra recorded with $t_{\text{mix}}=12$ ms is most sensitive to diffusion coefficients D between 0.4×10^{-12} and 1.5×10^{-12} m^2/s ($\tau_D=42$ ms and 11.4 ms) whereas for $t_{\text{mix}}=2$ ms this range is between $D=2\times10^{-12}$ and 5×10^{-12} m^2/s ($\tau_D=8.5$ ms and 3.4 ms).

E. Restricted diffusion on a sphere

To estimate the effect of gel domains on the effective diffusion coefficient, a simple domain model is suggested here. It is based on the solution of the spherical diffusion equation with a special boundary condition to model a diffusion barrier with reflecting boundaries. The model assumes fluid domains of equal sizes, with spherical, reflecting diffusion barriers between gel and liquid phase. For the mathematical treatment, one can restrict the consideration to a single spherical diffusion barrier around the south pole of a sphere (Fig. 2). The boundary of this barrier is at $\Omega_b=(\pi-\theta_b,\varphi)$. First the propagator $P(\Omega_1,\Omega_2,t=t_m)$ for diffusion on a sphere has to be calculated, which represents the probability for a molecule that is initially ($t=0$) at a position $\Omega_1=(\theta_1,\varphi)$ to diffuse to a position $\Omega_2=(\theta_2,\varphi)$ during the mixing time t_m. $P(\Omega_1,\Omega_2,t=t_m)$ for restricted diffusion in the context of this domain model can be calculated from the following boundary value problem:

$$\frac{\partial c(\Omega,t)}{\partial t}=D_0\Delta c(\Omega,t), \tag{2}$$

$$c(\Omega,t=0)=\delta(\Omega-\Omega_1), \tag{3}$$

$$\frac{\partial c(\Omega,t)}{\partial \Omega}=0 \quad \text{at } \Omega=\Omega_b=(\pi-\theta_{b,\varphi}). \tag{4}$$

TABLE I. Temperature dependence of the diffusion coefficient D in DMPC-$d9$ solid supported bilayers (SSV) with a radius of 320 nm. D was determined from the diagonal ratio of 2D-exchange spectra recorded at mixing times of 2 and 4 ms using the procedure described in Sec. II E.

T (°C)	25	30	35	37	42	45	50
$D(t_m=2\ \text{ms})$ $(10^{-12}\ \text{m}^2/\text{s})$	4.1±0.3	4.6±0.4	5.3±0.9	5.8±0.9	9.3±1.2	9.9±1.2	10.5±1.2
$D(t_m=4\ \text{ms})$ $(10^{-12}\ \text{m}^2/\text{s})$	4.9±0.9	5.2±0.9	5.4±0.9	5.7±0.9	8.5±1.2		

$c(\Omega,t)$ describes the concentration at the position Ω at time t provided that all molecules were initially at a position Ω_1 and are diffusing with a diffusion constant D_0. Δ is the Laplacian operator in spherical coordinates and $P(\Omega_1,\Omega_2,t_m)$ is given by $c(\Omega_2,t_m)$. Equation (4) describes the reflecting boundary of the barrier with an opening angle of θ_b (cf. Fig. 2). This boundary value problem is solved numerically, as described in the Appendix.

From $P(\Omega_1,\Omega_2,t_m)$ we can now calculate the mean-squared diffusion length $\langle r^2\rangle$ during the mixing time t_m in the presence of this diffusion barrier:

$$\langle r^2\rangle = \int\int d(\Omega_1,\Omega_2)^2 p(\Omega_1) P(\Omega_1,\Omega_2,t_m) d\Omega_1 d\Omega_2 . \tag{5}$$

$p(\Omega_1)$ is the *a priori* probability of the starting position Ω_1 and $d(\Omega_1,\Omega_2)$ is the distance between the starting position Ω_1 and the final position Ω_2 over the surface of the sphere. Then the effective diffusion coefficient D_{eff} can be calculated in the following way:

$$D_{\text{eff}} = \langle r^2\rangle / 4t_m . \tag{6}$$

D_{eff} is lowered compared to the free diffusion coefficient due to the effect of the diffusion barrier at $\Omega_b=(\pi-\theta_b,\varphi)$. To obtain a measure for the influence of the diffusion barrier it is useful to calculate the ratio between the effective diffusion coefficient D_{eff} and the coefficient D_0 for free, unrestricted diffusion at the same temperature. The relative (normalized) diffusion coefficient D_{rel} is defined by

$$D_{\text{rel}} = D_{\text{eff}} / D_0 . \tag{7}$$

A good parameter for describing the dependence of the relative diffusion coefficient D_{rel} on the size of the diffusion barrier is the ratio between the diameter b_f (cf. Fig. 2) of the fluid domain and the diffusion length l_D in the absence of diffusion obstacles where l_D is defined by

$$l_D = \sqrt{4 t_m D_0} . \tag{8}$$

III. RESULTS

Two bilayer systems were studied. As a first step, pure DMPC-$d9$ single bilayers on a spherical silica support (320± 20 nm radius) were measured at various temperatures and at two mixing times t_m using the 2D-NMR. These measurements are a prerequisite for the experiments in binary systems to test the reliability of the quantitative analysis method applied for the determination of the lateral diffusion constant D and to obtain D values for a bilayer system that is homogeneous above its phase-transition temperature (spatially unrestricted lateral diffusion). As a second step we applied the same methods for studying D in the coexistence region of an equimolar DMPC-DSPC mixture at various t_m (2, 4, 6, and 12 ms) and temperatures (28–45 °C).

A. Pure DMPC bilayers on a spherical support

Owing to the well-defined geometry and diameter of our sample, the experimental diagonal ratio determined as described above [Fig. 1(a)] can be used together with the theoretical calibration curve [Fig. 1(b)] for a direct determination of D at the temperature of the measurement. This is true as long as lateral diffusion on the spherical surface is the dominating motional process. The results are shown in Table I. We denote this diffusion coefficient that results from unrestricted diffusion over the spherical surface as D_0. The larger error of D_0 at higher temperatures and the longer (4 ms) mixing time t_m arises from the fact that for a certain t_m there is only a limited range of diffusion coefficients where the diagonal ratio is most sensitive (cf. Sec. II D). For $t_m=2$ ms the sensitive range is approximately $(2-7)\times10^{-12}$ m^2/s while for $t_{\text{mix}}=4$ ms it is $(1.5-3)\times10^{-12}$ m^2/s.

B. Spherical supported bilayers of 1:1 (mol) DMPC/DSPC

A differential scanning calorimetry (DSC) scan of the equimolar DMPC-$d9$–DSPC mixture as a single bilayer on the same spherical support as used above for DMPC is shown in Fig. 4 (ascending temperature mode). This broad and complex endothermic feature gives a liquidus temperature $T_L=43$ °C and a solidus temperature $T_S=22$ °C and indicates a significant demixing in the gel phase at $T<T_S$. The values of T_S and T_L are 4.5 °C lower than expected from the phase diagram of a MLV DMPC-DSPC mixture [22] but the temperature difference between the two peaks is exactly the same as obtained for MLV. This lowering of the transition temperatures is typical for single bilayers on a spherical support and results from lateral tension of the bilayer in the gel phase [16]. Thus, the modified phase diagram for supported bilayers can be obtained by reducing the MLV values of liquidus and solidus temperatures given in [22] by 4.5 °C DSC measurements of supported bilayers performed at DMPC-DSPC molar ratios of 1:3 and 3:1 confirmed this approximation.

2D experiments were performed in the temperature range of 25 ° to 45 °C at four different mixing times ($t_m=2$, 4, 6, and 12 ms) as described in Sec. II B. Representative contour

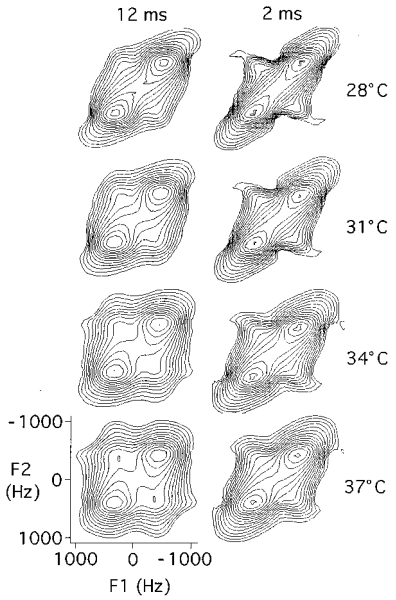

FIG. 3. Contour plots of 2D-exchange NMR spectra of an equimolar mixture of DMPC-*d*9–DSPC as single bilayers on a spherical solid support with a radius $R=320$ nm recorded with mixing times of $t_m=2$ and 12 ms at temperatures of 28, 31, 34, and 37 °C.

plots of the experimental 2D spectra (Fig. 3) for $t_m=2$ and 12 ms are shown in Fig. 3 for various temperatures. The change of the diagonal ratio with t_m is obvious for all temperatures.

Quantitative analysis of the spectra in terms of a lateral diffusion coefficient D was achieved by employing the same semiempirical approach that was used above for the pure DMPC data (cf. Sec. II D). However, it should be noted that now, owing to the coexistence of fluid and solid domains below the liquidus point of the mixture, lateral diffusion may be hindered by the presence of solid domains, resulting in an effective diffusion coefficient $D_{\text{eff}} \leqslant D_0$. The values obtained for D_{eff} by this approach are summarized in Table II for all temperatures studied together with the relative gel phase area at this temperature deduced from the modified DMPC-DSPC phase diagram using 48 and 52 Å^2 as gel phase area per DMPC and DSPC molecule.

As expected from the contour plots in Fig. 3, significant differences of D_{eff} are obtained for different mixing times at a given temperature. The value of D_{eff} is highest at the shortest $t_m=2$ ms and decreases (in some cases by more than 50%) for the longest $t_m=12$ ms at the same temperature T. A convenient way to get a measure for the reduction of lateral diffusion by the gel domains is to normalize D_{eff} by D_0, the lateral diffusion coefficient of DMPC obtained for the pure DMPC supported bilayer at the same temperature. Thus, D_0 represents the case of unrestricted diffusion in a homogeneous fluid phase bilayer. Values of D_0 at the corresponding temperature are listed in Table II. The resulting relative diffusion coefficient $D_{\text{rel}}=D_{\text{eff}}/D_0$ is plotted vs T in Fig. 4 for all mixing times studied. To facilitate the assignment of temperatures to the position in the coexistence region, we have additionally included the DSC endotherm of the equimolar mixture in Fig. 4. A drastic dependence of D_{rel} on both T and t_m can be observed. For high temperatures $T>T_L=43$ °C, D_{rel} is close to unity for short t_m, indicating largely unrestricted diffusion. Note that only t_m values of 2 and 4 ms are suitable for measuring the unrestricted diffusion, since longer t_m are prone to insensitivity for these high values of D as discussed above (Sec. II D). At temperatures within the coexistence region, D_{rel} decreases drastically with T for long t_m while this reduction is almost negligible for $t_m=2$ ms. As an example, at 38 °C, D_{rel} has dropped to 60% of its initial value for $t_m=12$ ms while for $t_m=2$ ms the reduction is less than 10%. This is even more obvious for 33 °C, where all t_m give significantly different values of D_{rel} with the longest mixing time being most sensitive to the slowdown of diffusion by the gel domain obstacles. At 28 °C, diffusion measured at $t_m=12$ ms comes virtually to a halt.

The validity of our D_{rel} vs T data for longest mixing time (12 ms) is confirmed by an independent measurement of the

TABLE II. Temperature dependence of the effective diffusion coefficient D_{eff} of 1:1 DMPC-*d*9–DSPC in solid supported bilayers (SSV). D_{eff} was determined from 2D exchange experiments with mixing times t_m of 2, 4, 6, and 12 ms from the ratio of the diagonals using the procedure described in Sec. II E. D_0 is the diffusion coefficient for free diffusion of DMPC-*d*9 at this temperature without diffusion barriers. It is estimated from D in the homogeneous fluid phase (45 °C) by extrapolation to lower T using the temperature dependence of D in DMPC-*d*9 SSV. The relative gel area was determined from the modified DMPC-*d*9–DSPC phase diagram.

T (°C)	$t_m=2$ ms (10^{-12} m^2/s)	$t_m=4$ ms (10^{-12} m^2/s)	$t_m=6$ ms (10^{-12} m^2/s)	$t_m=12$ ms (10^{-12} m^2/s)	Relative gel area	D_0 (10^{-12} m^2/s)
25					0.71	3.5
28				0.3±0.05	0.68	3.8
31.5		2.7±0.12	1.8±0.1	1.2±0.1	0.56	4.1
33	4.0±0.2	3.0±0.12	2.3±0.1	1.5±0.4	0.52	4.4
34.5	4.3±0.2	3.4±0.5	2.9±0.6		0.46	4.7
36.5	4.6±0.2	4.1±0.5	3.7±0.6	2.5±0.4	0.39	5.2
38	5.0±0.2	4.6±0.5	4.0±0.6	3.4±0.4	0.32	5.7
40	5.2±0.5	5.0±0.5	4.1±0.6		0.23	6.0
41.5	6.3±0.6	5.9±0.5			0.12	6.3
43	6.6±0.6	6.1±0.6			0	6.9
45	7.0±0.6				0	7.5

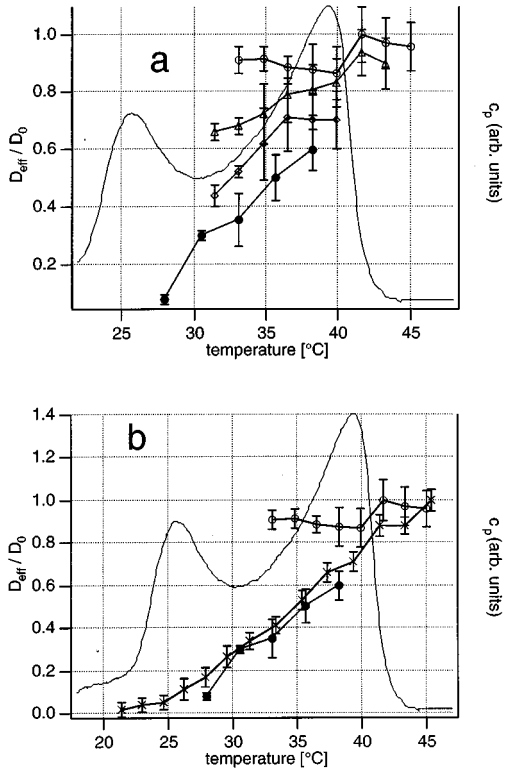

FIG. 4. (a) Temperature dependence of the relative diffusion coefficient $D_{rel}=D_{eff}/D_0$ of (1:1) DMPC-$d9$–DSPC single bilayers on a spherical support measured by 2D-NMR at $t_m=2$ (○), 4 (△), 6(◇), and 12 ms (●). The DSC endotherm of the mixture is shown by a broken line. (b) D_{ref} vs T for a DMPC-$d54$–DSPC-$d70$ mixture measured with the SFF 1H-NMR technique (×). For comparison, the data from (a) for $t_m=2$ and 12 ms and the DSC endotherm are shown. The solidus and liquidus temperatures of the two systems are comparable.

same lipid mixture using the recently introduced SFF technique. Note that planar-oriented lipid multilayers on glass plates were used for this measurement; therefore the support itself gives no restrictions to the diffusion.

SFF is analogous to a pulsed-field gradient proton NMR experiment, but the gradient is produced by the fringe field of the superconducting NMR magnet and the pulse effect is obtained by employing the stimulated echo sequence [14]. This enables extreme stable field gradients of more than 50 T/m and thus an experimental length scale of ≈ 1 μm that is comparable to that of the 2D exchange method at $t_m=12$ ms. Figure 4(b) shows the SFF results together with the data from Fig. 4(a) for $t_m=2$ and 12 ms as a function of temperature. For this comparison the SFF data have been subjected to a 2 °C shift to lower temperatures to account for the general reduction of the phase transition in single bilayers on a spherical support [16,23] compared to planar multilayers. There is an excellent agreement between the SFF data and the 2D data for $t_m=12$ ms while the data for $t_m=2$ ms agree with the SFF results only above T_L but show higher D_{rel} within the coexistence region.

IV. DISCUSSION

A. Unrestricted diffusion in pure DMPC

A good consistency check of the data analysis method applied is a comparison of our results with those obtained by other methods. We obtain $D_0=(4.1\pm0.3)\times10^{-12}$ m^2/s ($t_{mix}=2$ ms) and $D_0=(4.8\times0.9)\times10^{-12}$ m^2/s ($t_{mix}=4$ ms) at a temperature of 25 °C. These values and the temperature dependence of D (Table I), giving an activation energy of 28 ± 7 kJ/mol, are in excellent agreement with values measured by Vaz, Clegg, and Hallmann [2] using fluorescence methods (FRAP) and also with those obtained by pulsed-field gradient NMR measurements [3]. Moreover, it is noteworthy that no dependence of D on t_m is observed for the case of pure DMPC, as is expected for an unrestricted diffusional motion.

The good agreement of our D_0 data for unrestricted diffusion with those obtained by other methods gives us the necessary confidence that the semiempirical approach for analyzing the 2D-NMR data is justified and reliable. The result provides additional evidence that under the given experimental conditions diffusion is indeed the dominating motional process in the bilayer. Thus, we are now ready to use this method for studying restricted diffusion in binary lipid mixtures. It should be emphasized that this is possible only owing to the well-defined geometry of the samples, which enables a direct comparison of theoretical and experimental 2D spectra.

B. Restricted diffusion in 1:1 DMPC-DSPC

1. Domain distance and experimental length scale

A major difference between the D_0 values measured for pure DMPC and the D_{eff} values of the mixture in the coexistence region is that D_{eff} only shows a marked dependence on the t_m value (Fig. 4) and thus on the experimental length scale over which the diffusion is averaged. This indicates that obstacles exist in the mixture that give a significant hindrance to unrestricted lateral diffusion. The formation of gel phase domains inside of which D is virtually frozen is the most likely origin of such obstacles. Their formation starts spontaneously at temperatures in the vicinity of T_L as extremely small clusters of gel phase molecules, containing preferentially the high melting DSPC, and floating in a matrix of fluid phase, DMPC enriched mixture. With decreasing temperature, the size or the number of the domains (and thus the total gel phase area, cf. Table II) increases and the average size of the fluid domains decreases.

The exact composition of gel domains and fluid phase can be extracted from the phase diagram of the mixture using the lever rule. We note that in our 2D-NMR experiments DSPC does not contribute to the spectrum since only DMPC is deuterated. Moreover, all DMPC bound in a gel domain does not contribute any off-diagonal intensity to the 2D spectrum, since diffusion in gel domains is at least two orders of magnitude slower and thus outside the sensitive time window of the experiment. This can be seen for 2D spectra measured at $t_m=12$ ms and at temperatures ($T=23$ °C) where more than 80% of the DMPC is in the gel phase. Since the selection of t_m in a 2D-NMR experiment permits us to vary the length scale of the experiment, the diffusion measurement will be influenced by the domains when the diffusion length l_D [Eq. (8)] approaches the average fluid domain size corresponding to b_f in our very simple domain model (Fig. 2). Considering the t_m values used in our measurements, the experimental length scale varies from 100 to 600 nm, estimated on the

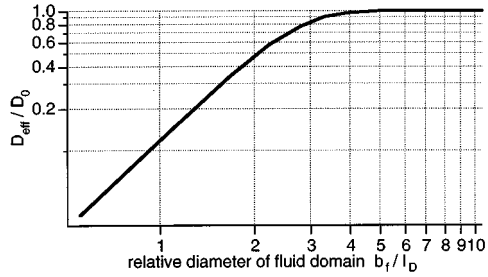

FIG. 5. Numerical simulation of D_{rel} vs the ratio between fluid domain size b_f and the diffusion length l_D in terms of the domain model shown in Fig. 2.

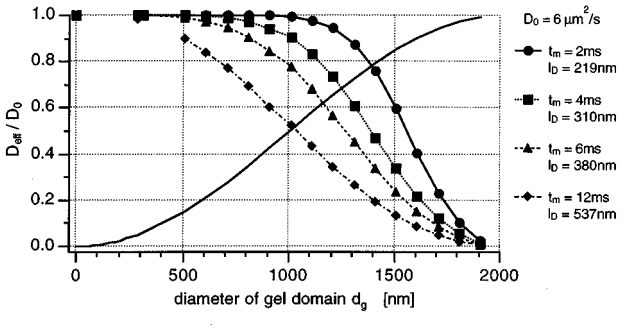

FIG. 6. Numerical calculation of D_{rel} vs d_g for different mixing times t_m together with the area contribution of gel phase at $D_0 = 6\times10^{-12}$ m^2/s for our model.

basis of l_D for unrestricted diffusion.

Since D_{eff} obtained for $t_m = 2$ ms is barely affected by a decrease of T (Fig. 4), we can now estimate ≈ 200 nm (42 °C) and ≈ 100 nm at 30 °C as a *lower* limit for the average fluid domain size using Eq. (8) and the values of D_0. These values are in reasonable agreement with those estimates reached by other methods, but for different systems. The approximation $D_{\mathrm{eff}} \approx D_0$ for the diffusion between the domains is justified by the fact that $D_{\mathrm{rel}} \approx 1$ for $T > T_L$ (Fig. 4).

2. Domain size

While domains in lipid monolayers exhibit diameters in the μm range and can be readily observed by fluorescence microscopic methods, a direct measurement of the presumably much smaller domains in bilayers has not been reported yet, besides some electron microscopy work to be discussed below. All other experimental estimates of bilayer domain sizes published so far used indirect methods of measurement together with a suitable domain model.

Our domain model introduced in Sec. II D (Fig. 2) is certainly an oversimplification but it allows us to make use of the well-known sample geometry in our experiment and of the simulations in order to obtain an upper limit for the gel and fluid domain sizes d_g and b_f. Assuming hard, reflecting domain edges without any boundary layer and a sphere radius of 320 nm as used in the measurements, we obtain by numerical calculation a dependence of $D_{\mathrm{rel}} = D_{\mathrm{eff}}/D_0$ on the relative diameter of the fluid regions b_f/l_D as shown in Fig. 5. Hence the case of unrestricted diffusion ($D_{\mathrm{rel}} \approx 1$) is given for $b_f/l_D > 5$ while restricted diffusion is evident for $b_f < 2l_D$. Therefore a measurement with different t_m can provide the required information about b_f only for fluid domain dimensions less than twice l_D within our simple model.

Figure 6 shows the results of the numerical calculation of D_{rel} vs d_g for different mixing times together with the area contribution of gel phase at $D_0 = 6\times10^{-12}$ m^2/s for our model. It clearly shows that the 2D-NMR experiment becomes sensitive for the presence of gel domains as a diffusion obstacle above a certain critical domain size that depends on t_m. The most sensitive case is $t_m = 12$ ms where gel domains should be detectable at $d_g > 500$ nm, corresponding to a gel domain area of 20%. This indicates that an estimate of d_g within this model will provide exaggerated values that can only be considered as an upper limit. For $t_m = 12$ ms and $D_0 = 5.7\times10^{-12}$ m^2/s (Table II) corresponding to $l_D = 530$ nm [Eq. (8)], we obtain for $T = 38$ °C a value of $D_{\mathrm{rel}} = 0.6$ (Fig. 4) and thus $d_g = 900$ nm from Fig. 6.

The demonstration of the sensitivity of the NMR experiment for certain domain sizes at a given t_m and thus at a time or length scale adjustable by the experimenter, is probably the main virtue of our simple domain model. The values obtained for d_g would certainly be considerably lower assuming the existence of more than one gel domain per sphere. Further reduction is expected from assuming domains being elliptic, dendritic, or fractal in shape, which seems closer to the reality.

Another model of the effect of circular domains as obstacles for diffusion has been suggested by Almeida, Vaz, and Thompson [12] on the basis of FRAP data of 1:1 DMPC-DSPC mixtures. It considers immobile gel domains of constant diameter with a boundary region characterized by a screening length $\xi = 10-22$ Å between fluid and gel state. Using our values of D_{rel} for $t_m = 12$ ms gives $d_g = 30-66$ nm according to this model. However, it should be pointed out that an underestimate of d_g is likely here since this model assumes a constant domain diameter at all temperatures and gel area fractions. To explain a decrease in D_{rel} an increasing proportion of boundary region of the domains is needed, thus requiring low values of d_g. Furthermore, no consideration is given to the influence of different experimental time and length scales within this model.

A model which explicitly considers a temperature dependence of d_g for MLV dispersions of 1:1 DMPC-DSPC has been used to estimate domain sizes from ESR line-shape analysis of the signal arising from the spin labeled DMPC, giving $d_g \leqslant 20$ nm above the percolation threshold [13].

Hence all these models predict domain sizes of approximately one order of magnitude below our estimate for the upper limit of d_g. On the other side, domains of sizes 0.2–0.5 μm in single planar bilayers of 1:1 DLPC-DPPC on a solid support were directly visualized using electron microscopic techniques [24] and even larger domain structures were observed by fluorescence techniques in fibroplast membranes [25].

3. Domain connectivity and percolation

Decreasing T of the mixture over the coexistence region has been demonstrated in previous work to cause a disconnection of the previously continuous fluid and DMPC-rich areas of the bilayer, i.e., a transition from a disconnected gel

to a disconnected fluid takes place at a disconnection temperature T_D within the coexistence region [11,13,26]. The average diameter b_f of the fluid domains may ultimately become less than l_D and thus the value of D_{rel} should exhibit a drop for temperatures where $b_f < l_D$. This was observed by FRAP [11,26] and ESR [13] and both methods identified the disconnection point for the 1:1 mixture at $T_D = 43 \pm 2$ °C and at a fluid phase area fraction of 0.73. This temperature would correspond to $T = 38.5 \pm 2$ °C for our mixture considering the above-mentioned 4.5 °C temperature correction for single bilayers on a spherical support. However, it is quite clear from both our 2D-NMR and SFF data in Fig. 4 that no disconnection can be observed at mixing times t_m corresponding to a l_D of 600 nm–1 μm. Our values of D_{rel} show a largely linear decrease with T down to 25 °C rather than a sharp drop at T_D as observed by FRAP and ESR. A similar linear decrease of D_{rel} is reported for a FRAP measurement in a Ceramide-DPPC mixture [27] above the percolation threshold and was interpreted as restricted diffusion in an archipelago of inpermeable domains as mobile obstacles [28].

On the other side, the good agreement between our SFF and 2D-NMR data and the fact that both methods do not rely on the use of labels that change the packing properties of the lipids as fluorescence and spin labels do, makes us confident that our results reflect, indeed, the true diffusional behavior in the coexistence region. Furthermore, the agreement of the SFF and 2D-NMR data effectively rules out the possibility that exchange of DMPC between the fluid and gel domains gives a major contribution to the 2D-NMR results. SFF is not sensitive to this type of exchange since only spatial displacements along the gradient will be detected. Neither can the sample geometry account for this result since the SFF method uses planar multilayers similar to the FRAP experiment while the 2D-exchange method uses single bilayers on a spherical support. Our results indicate that either a disconnection or percolation does not take place or that the size of the disconnected fluid must be larger than ≈ 1 μm at all temperatures above 28 °C assuming immobile obstacles during the mixing time t_m. The most likely explanation for this unexpected result is that the observation of a disconnection point must relate to the experimental time and length scale of the method applied. While our NMR methods sample over maximum distances of 600 and 1 μm ($t_m = 12$ ms and the SFF method), FRAP methods measure over several μm. This may explain why diffusion observed by FRAP appears to be restricted at a point where unrestricted diffusion is seen by the NMR methods. The disconnection may then manifest itself by an abrupt drop of D_{rel} for FRAP while it shows by a rather continuous reduction of D_{rel} with decreasing T at length scales that are one magnitude shorter. This is further supported by the finding that at $t_m = 2$ ms (i.e., $l_D \approx 100$ nm at 30 °C) no significant reduction of D_{rel} can be observed down to 30 °C while the reduction is quite obvious for $t_m = 12$ ms.

The length scale of the intrinsically sub-ns-time-scale-sensitive ESR method is obscured by the rather complex line-shape analysis and the numerous assumptions put in there [13]. The most severe constraint might be the focusing to the slow exchange limit while the possibility of intermediate exchange of spins between fluid and gel was not considered. Therefore we cannot assign this method to a characteristic time or length scale but the similarity between ESR and FRAP results suggests that this must be also in the μm region.

Another, more remote possibility is that the lipids with the bulky fluorescence and spin labels attached exhibit a diffusion behavior different from the bulk owing to their modified packing in the bilayer. This could be of particular importance when considering the boundary region between gel and fluid. Such regions are rich in defects and thus in free volume that may cause an enrichment of fluorescence or spin labeled lipids that itself represent a certain packing constraint. They may diffuse readily along the boundary before they return to the bulk. In such a case, a disconnection would have a profound effect on D_{rel} since now a significant proportion of labeled lipids would be confined at the boundary of a disconnected fluid. On the other side, the largely unlabeled lipids (note that selective deuteration does not pose any packing constraint) used for NMR are more likely to behave like the bulk and thus should not show any special affinity for the boundary region. This effect should be particularly severe when the geometry of the boundary changes in the vicinity of T_D from a simple and smooth one above T_D to a complicated and rough one below T_D (e.g., a fractal shape). Then diffusion along the boundary would be much less efficient than the motion within the fluid bulk of the disconnected domain.

Finally, we have to consider the effect of the mobility and the shape of the domains on T_D since percolation can be observed strictly only under conditions of obstacles being immobile during the experimental time scale as given by t_m for our methods. Monte Carlo lattice simulations done by Saxton [28,29] have clearly shown that T_D decreases for increasing domain mobility, i.e., the percolation threshold is shifted towards larger area fractions of gel phase. In the limit of a domain mobility comparable to the D_0 in the mixture, T_D will coincide with the solidus temperature T_S. Thus, a high domain mobility might well account for not observing percolation by NMR but the question remains why FRAP with its even longer time scale is sensitive to percolation. It could be that the domains perform some local motion on a short time scale or even a fluctuation of their boundary at correlation times in the range of the NMR experiment but which is averaged out at the FRAP time scale. In a similar way, a rapid exchange of DMPC between the gel phase boundary and the fluid bulk would be a mechanism that may shift T_D downward. In contrast, the FRAP probe molecule would not undergo such an exchange since it partitions exclusively into the fluid phase.

The effect of domain shape on percolation has been treated theoretically in terms of a continuum simulation model of random freely overlapping ellipses as a function of their semiaxis ratio in [30]. It was found that highly eccentric ellipses disconnect the matrix at a smaller area fraction than nearly circular obstacles would do. In the light of our results this would suggest that the domains must appear highly elongated for the fluorescence probe molecule at the FRAP time scale while being more circular on the NMR time scale. Such a condition is certainly hard to satisfy.

V. CONCLUSION

We have shown that 2D-exchange NMR can be used to measure lipid diffusion in the coexistence region of a binary

mixture and that these methods allow the variation of the experimental length scale by adjusting the mixing time t_m. The shorter the length scale, the less sensitive becomes the diffusion measurement for the presence of domains as obstacles for unrestricted diffusion. The finding that 2D-exchange NMR does not detect any indication of a disconnection above 28 °C (which is supported by the SFF method) is in contrast to previous FRAP and ESR results. SFF studies at longer mixing times and thus at length scales comparable to the FRAP method might be able to resolve this discrepancy. However, the results seem to teach us that the discussion of disconnection phenomena always requires a thorough consideration of the time and length scales of the experimental methods applied as well as of the disturbances that the probe molecules may have on their surrounding.

APPENDIX: RESTRICTED DIFFUSION IN A SIMPLE GEL-DOMAIN MODEL

To obtain the propagator for restricted diffusion in the domain model described in Sec. II E [Eq. (4)] the Laplacian is discretized and the boundary value problem is solved numerically. The θ-dependent part of the Laplacian Δ in spherical coordinates $\Omega=(\theta,\varphi)$ is given by

$$\Delta=\frac{1}{R^2}\frac{1}{\sin\theta}\frac{\partial}{\partial\theta}\left(\sin\theta\,\frac{\partial}{\partial\theta}\right). \tag{A1}$$

The angle θ is discretized in the following way:

$$\theta_i=(i-\tfrac{1}{2})\Delta\theta \quad \text{with} \quad \Delta\theta=\pi/N. \tag{A2}$$

N is the number of sites in θ and $\Delta\theta$ is the resolution of the discretization. The discrete version of the propagator $P(\Omega_1,\Omega_2,t=t_m)$ is now a $N\times N$ matrix $\mathbf{P}(i_1,i_2|t_m)$. The elements of $\mathbf{P}(i_1,i_2|t_m)$ contain the probability for a jump from site i_1 to i_2 during the mixing time t_m. Equation (A2) can then be written as a matrix equation:

$$\frac{d}{dt}\mathbf{P}=\Pi\mathbf{P}. \tag{A3}$$

$\mathbf{P}$ is the matrix of the propagator and Π is the discretized Laplace operator. The kinetic matrix Π can be determined by replacing the spatial derivatives by their corresponding difference equation. Π is tridiagonal with the diagonal elements $\Pi(i,i)$ and the subdiagonals $\Pi(i\pm1,i)$ [31,32]:

$$\Pi(i\pm1,i)=\frac{1}{6\tau_D(\Delta\theta)^2}\frac{\sin(\theta_i\pm\frac{1}{2}\Delta\theta)}{\sin\theta_i}, \tag{A4}$$

$$\Pi(i,i)=\frac{1}{6\tau_D(\Delta\theta)^2}\cos(\tfrac{1}{2}\Delta\theta). \tag{A5}$$

τ_D is the diffusion correlation time as defined by Eq. (A1) and the indices in Π must be restricted to the range from 1 to N. $\Pi(i,j)$ describes the rate at which diffusion jumps occur between sites i and j. A formal solution of the diffusion equation [Eq. (A10)] can be written in the following way:

$$\mathbf{P}=\exp(\Pi t_m)\mathbf{P}_0. \tag{A6}$$

$\mathbf{P}_0$ is given by the initial condition [Eq. (A3)] as

$$\mathbf{P}_0(i,j)=\mathbf{P}(i,j|t=0)=\delta_{i,j}p(\theta_i), \tag{A7}$$

where $p(\theta_i)$ is the probability for having an initial orientation of θ_i. Thus in the case of a powder sample $\mathbf{P}_0$ is given by

$$\mathbf{P}_0(i,j)=\delta_{i,j}\sin[(i-\tfrac{1}{2})\Delta\theta]\sin\left(\frac{\Delta\theta}{2}\right). \tag{A8}$$

Solving Eq. (A6) is equivalent to finding the eigenvalues of the following symmetric matrix $\mathbf{S}$ [32,33]:

$$\mathbf{S}=\mathbf{P}_0^{-1/2}\Pi\mathbf{P}_0^{1/2}. \tag{A9}$$

Hence the problem is reduced to finding the eigenvalues of a real and symmetric tridiagonal matrix, which can be solved by standard numerical procedures. The solution for the propagator $\mathbf{P}(i_1,i_2|t_m)$ is then

$$\mathbf{P}=[\mathbf{P}_0^{1/2}\mathbf{M}]\exp(\lambda t_m)[\mathbf{P}_0^{1/2}\mathbf{M}]^T, \tag{A10}$$

where $\mathbf{M}$ is the matrix containing all eigenvectors of $\mathbf{S}$, λ is a vector with all N eigenvalues of $\mathbf{S}$ and t_m is the mixing time.

To describe diffusion between the reflecting barriers properly one has to incorporate the boundary condition [Eq. (A4)] into the kinetic matrix [31,34–36]. If there is a reflecting barrier at θ_k, the element $\Pi(k,k)$ has to be modified as follows:

$$\Pi(k,k)=\frac{1}{3\tau_D(\Delta\theta)^2}\cos(\tfrac{1}{2}\Delta\theta). \tag{A11}$$

The subdiagonals are defined as in Eq. (A4).

[1] P. F. F. Almeida and W. L. C. Vaz, in *Structure and Dynamics of Membranes. From Cells to Vesicles*, edited by R. Lipowsky and E. Sackmann (Elsevier, Amsterdam, 1995), pp. 305–357.

[2] W. L. C. Vaz, R. M. Clegg, and D. Hallmann, Biochemistry **24**, 781 (1985).

[3] A.-L. Kuo and C. G. Wade, Biochemistry **18**, 2300 (1979).

[4] T. Köchy and T. M. Bayerl, Phys. Rev. E **47**, 2109 (1993).

[5] C. Dolainsky, M. Unger, M. Bloom, and T. M. Bayerl, Phys. Rev. E **51**, 4743 (1995).

[6] Y. K. Shin and J. H. Freed, Biophys. J. **55**, 537 (1989).

[7] Y. K. Shin, U. Ewert, D. E. Budil, and J. H. Freed, Biophys. J. **59**, 950 (1991).

[8] P. Deveaux and H. M. McConnell, J. Am. Chem. Soc. **94**, 4475 (1972).

[9] S. König, E. Sackmann, D. Richter, R. Zorn, C. Carlile, and T. M. Bayerl, J. Chem. Phys. **100**, 3307 (1994).
[10] S. König, T. M. Bayerl, G. Coddens, D. Richter, and E. Sackmann, Biophys. J. **68**, 1871 (1995).
[11] W. L. C. Vaz, E. C. C. Melo, and T. E. Thompson, Biophys. J. **56**, 869 (1989).
[12] P. F. F. Almeida, W. L. C. Vaz, and T. E. Thompson, Biochemistry **31**, 7198 (1992).
[13] M. J. Saxton, Biophys. J. **61**, 119 (1992).
[14] P. Karakatsanis and T. M. Bayerl, Phys. Rev. E **54**, 1785 (1996).
[15] S. König, W. Pfeiffer, T. Bayerl, D. Richter, and E. Sackmann, J. Phys. (France) II **2**, 1589 (1992).
[16] C. Naumann, T. Brumm, and T. M. Bayerl, Biophys. J. **63**, 1314 (1992).
[17] T. Brumm, K. Jorgensen, O. Mouritsen, and T. M. Bayerl, Biophys. J. **70**, 1373 (1996).
[18] C. Schmidt, B. Blümich, and H. W. Spiess, J. Magn. Reson. **79**, 269 (1988).
[19] C. Dolainsky, A. Möps, and T. M. Bayerl, J. Chem. Phys. **98**, 1712 (1993).
[20] A. Hagemeyer, L. Brombacher, K. Schmidt-Rohr, and H. W. Spiess, Chem. Phys. Lett. **167**, 583 (1990).
[21] D. B. Fenske and H. C. Jarrell, Biophys. J. **59**, 55 (1991).
[22] W. Knoll, K. Ibel, and E. Sackmann, Biochemistry **20**, 6379 (1981).
[23] T. Brumm, O. Mouritsen, K. Joergensen, and T. M. Bayerl, Biophys. J. **70**, 1373 (1996).
[24] S. W. Hui, Curr. Top. Membr. Transp. **29**, 29 (1987).
[25] E. Yechiel and M. Edidin, J. Cell Biol. **105**, 755 (1987).
[26] W. L. C. Vaz, E. C. C. Melo, and T. E. Thompson, Biophys. J. **58**, 273 (1990).
[27] P. F. F. Almeida, W. L. C. Vaz, and T. E. Thompson, Biochemistry **31**, 6739 (1992).
[28] M. J. Saxton, Biophys. J. **56**, 615 (1989).
[29] M. J. Saxton, Biophys. J. **52**, 989 (1987).
[30] W. Xia and M. F. Thorpe, Phys. Rev. A **38**, 2650 (1988).
[31] R. D. Richtmyer and K. W. Morton, *Difference Methods for Initial Value Problems* (Wiley, New York, 1967).
[32] S. Wefing, S. Kaufmann, and H. W. Spiess, J. Chem. Phys. **89**, 1234 (1988).
[33] K. Schmidt-Rohr and H. W. Spiess, *Multidimensional Solid State NMR and Polymers* (Academic, London, 1994), p. 320.
[34] M. H. Blees, J. Magn. Reson. **109**, 203 (1994).
[35] J. Kärger, H. Pfeiffer, and W. Heink, Adv. Magn. Reson. **12**, 1 (1988).
[36] G. P. Zientara and J. H. Freed, J. Chem. Phys. **72**, 1285 (1980).